



OPEN ACCESS

EDITED BY

Junchao Wei,
Nanchang University, China

REVIEWED BY

Elif Seven,
C-Dots Nanotec, LLC, United States
Yong Yang,
Northwestern Polytechnical University, China
Jiaolong Wang,
Affiliated Stomatological Hospital of Nanchang
University, China

*CORRESPONDENCE

Gisele Eva Bruch,
✉ gisele.bruch@professor.faminas.edu.br

RECEIVED 31 December 2023

ACCEPTED 25 September 2024

PUBLISHED 03 January 2025

CITATION

Bruch GE, Dal Bosco L, Cordeiro AP,
Cordeiro MF, Sahoo SK, Peixoto C,
Klosterhoff MC, Romano LA, Fantini C,
Santos AP and Barros DM (2025) Biodistribution
of intravenously delivered PEGylated carbon
nanotubes to the rat brain cortex.
Front. Carbon 3:1363919.
doi: 10.3389/frcarb.2024.1363919

COPYRIGHT

© 2025 Bruch, Dal Bosco, Cordeiro, Cordeiro,
Sahoo, Peixoto, Klosterhoff, Romano, Fantini,
Santos and Barros. This is an open-access
article distributed under the terms of the
[Creative Commons Attribution License \(CC BY\)](https://creativecommons.org/licenses/by/4.0/).
The use, distribution or reproduction in other
forums is permitted, provided the original
author(s) and the copyright owner(s) are
credited and that the original publication in this
journal is cited, in accordance with accepted
academic practice. No use, distribution or
reproduction is permitted which does not
comply with these terms.

Biodistribution of intravenously delivered PEGylated carbon nanotubes to the rat brain cortex

Gisele Eva Bruch^{1,2*}, Lidiane Dal Bosco^{1,3}, Arthur P. Cordeiro¹,
Marcos F. Cordeiro¹, Sangram K. Sahoo⁴, Carolina Peixoto¹,
Marta C. Klosterhoff⁵, Luis Alberto Romano⁵, Cristiano Fantini⁴,
Adelina P. Santos⁶ and Daniela M. Barros¹

¹Laboratório de Neurociências, Instituto de Ciências Biológicas, Universidade Federal do Rio Grande (FURG), Programa de Pós-graduação em Ciências Fisiológicas - Fisiologia Animal Comparada, FURG, Rio Grande, Brazil, ²Laboratório de Simulação Realística, Faculdade de Minas – Faminas BH, Belo Horizonte, Brazil, ³Universidade Federal do Pampa (UNIPAMPA), Uruguaiana, Brazil, ⁴Departamento de Física, Universidade Federal de Minas Gerais, Belo Horizonte, Brazil, ⁵Laboratório de Imunologia e Patologia de Organismos Aquáticos, Instituto de Oceanografia, Universidade Federal do Rio Grande, Rio Grande, Brazil, ⁶Centro de Desenvolvimento da Tecnologia Nuclear, CDTN, Belo Horizonte, Brazil

Polyethylene glycol-functionalized single-walled carbon nanotubes (SWCNT-PEG) have been studied for many biomedical applications because of their unique physicochemical properties. Due to their reduced size and high stability in physiological media, SWCNT-PEG are candidates for crossing the blood–brain barrier (BBB), with potential use in treating central nervous system diseases that are currently unresponsive to pharmacological interventions because of the tightly regulated permeability of the BBB. In this study, we investigated the biodistribution of intravenously delivered SWCNT-PEG using Raman spectroscopy, as well as possible toxicological outcomes using morphological, histological, biochemical, and behavioral analyses. SWCNT-PEG were identified in the brain cortex, blood, spleen, and liver of rats. Biochemical and histological analyses did not reveal toxic effects in rats 24 h after SWCNT-PEG injection. Additionally, no behavioral impairments were observed in treated animals subjected to the Morris water maze task. Our preliminary experimental results clearly indicate that SWCNT-PEG were able to cross biological membranes and reach the rat brain cortex parenchyma (but not other brain structures) after systemic administration without the presence of acute toxic effects. The biodistribution of SWCNT-PEG in a specific region of the brain tissue encourages further studies regarding the application of SWCNTs in neuroscience.

KEYWORDS

nanomedicine, carbon nanotubes, polyethylene glycol, biodistribution, Raman spectroscopy

1 Introduction

One of the greatest challenges in neuroscience is the search for an effective and non-invasive treatment for central nervous system (CNS) diseases. The efficacy of available treatments are limited because most therapeutic molecules are unable to permeate the brain parenchyma due to the blood–brain barrier (BBB) (Huang et al., 2017; Fernandes et al., 2018). The BBB is a complex physical and functional barrier that regulates the flux of blood-borne solutes into the brain, protecting the CNS from physical and chemical threats

(Irudayanathan et al., 2016; Pardridge, 2012). To overcome this problem, the use of nanomaterials has been proposed as a non-invasive strategy for the delivery of drugs across the BBB (Khongkow et al., 2019; Tam et al., 2016).

Among the various nanomaterials studied recently, carbon nanotubes (CNTs) have attracted immense interest in the neuroscience field, with promising results regarding BBB permeability and biosafety after local (Dal Bosco et al., 2015a; Dal Bosco et al., 2015b; Lee et al., 2011; Nunes et al., 2012) and systemic (Yang et al., 2007; Kafa et al., 2015; Kafa et al., 2016; Soligo et al., 2021) administration in rodents. Because of their small and controllable dimensions, unique physicochemical properties, and ease of chemical modification to improve biocompatibility either by covalent bonding (e.g., with polyethylene glycol—PEG) or by adsorption (e.g., with DNA), CNTs are considered strong candidates for many neurobiological applications. Furthermore, the unique properties of single-walled carbon nanotubes (SWCNTs), including their near-infrared photoluminescence with minimal tissue interference, make them ideal optical probes for biological applications (Fernandes et al., 2018).

Despite several possible applications of CNTs in biomedicine and neuroscience, much remains to be known about their biological implications. Although many studies have examined CNT effects using *in vitro* systems, there is a lack of information about the interactions of these materials with the CNS of animals under physiological conditions. It is thus essential to consider the importance of a detailed investigation of the effects of different types of CNTs (single walled—SWCNT and multi walled—MWCNT), with different levels of functionalization and purity, and diverse states of aggregation (Mann et al., 2022; Metternich et al., 2023).

Kafa et al. (2015) used two different methods to demonstrate the ability of MWCNTs to cross the BBB using a BBB co-culture *in vitro* model comprising primary porcine brain endothelial cells and primary rat astrocytes exposed to amino-functionalized MWCNTs, and an *in vivo* analysis consisting of the systemic administration of MWCNT radio-labelled with fluorescein isothiocyanate in mice. Another study showed that the intracerebroventricular injection of amine-modified SWCNTs resulted in brain protection from ischemic damage by reducing apoptosis, inflammation, and glial cell activation in a rat stroke model (Lee et al., 2011). In addition, studies using pristine SWCNTs (Yang et al., 2007), angiopep-2 targeted chemically-functionalized MWCNTs (Kafa et al., 2016), and Gd (L2) and Gd (L3) loaded onto different functionalized MWNTs (Costa et al., 2018) have been developed in order to enhance the biodistribution of CNTs and the ability to cross the BBB.

When in aqueous media, pristine SWCNTs tend to form aggregates that are associated with several toxic responses (Alshehri et al., 2016; Elsaesser and Howard, 2012; Kavosi et al., 2018; Pinals et al., 2020; Gravelly et al., 2022). One of the most successful strategies for overcoming this limitation is the functionalization of SWCNTs with PEG chains (SWCNT-PEG), which results in CNTs with more hydrophilicity and electrical neutrality (Dos Santos et al., 2007; Yang et al., 2020; Son et al., 2023; Lemos et al., 2023; Iverson et al., 2013). However, very little information is presently available regarding the rate and brain region-specific biodistribution of SWCNT-PEG in the CNS.

SWCNT-PEG are promising nanomaterials for many biomedical applications, thus requiring a better understanding of their behavior in biological systems (Zhu, 2017). Therefore, the aim of this study was to determine the presence of SWCNT-PEG in the CNS after intravenous injection in Wistar rats and to assess possible implications in spatial memory. We also investigated the presence of SWCNT-PEG in important organs for metabolism and excretion (liver, spleen, and kidney) and evaluated their interactions with the blood. Raman spectroscopy was used to detect nanotubes in the tissues because of its strong sensitivity based on resonance phenomena.

2 Results

2.1 Biodistribution

SWCNT-PEG distribution was assessed using Raman spectroscopy. SWCNT-PEG Raman signatures were observed in the liver, bone, blood, CNS (cerebral cortex), lung, and spleen (Figures 1A–F, respectively). The data provide direct evidence for the presence of SWCNT-PEG in the analyzed tissues. The detection of SWCNT-PEG was based on both the radial breathing mode (RBM) and tangential graphite-like phonon mode (G band). Our results show that, even though part of the nanomaterial accumulated in the liver and in the spleen, a considerable amount of CNTs were detected in the brain cortex.

2.2 Toxicity

To evaluate any potential toxic effects of SWCNT-PEG in the treated rats, we performed biochemical analyses of hepatic and renal key biomarkers. All tested parameters were within normal limits, not showing any obvious toxic effects in the liver or in the kidney after SWCNT-PEG treatment (Supplementary Figure S2).

We investigated the effects the presence of SWCNT-PEG in blood by assessing hematological parameters. The only variations observed were in the indexes for platelets and white blood cells, as there was a decrease in the number of platelets in the animals treated with higher concentrations of SWCNT-PEG (Table 1). Additionally, monocytosis and eosinophilia were observed in animals treated with the highest concentration of SWCNT-PEG (Figures 2A, B, respectively), while no differences were detected among treatments in the number of neutrophils, lymphocytes, and basophils (Figures 2C–E, respectively).

No toxic effects were detected based on necropsy, histology, and overall health (such as weight loss and fatigue) in rats injected with SWCNT-PEG. Similarly, histological analysis of the brain (Figure 3), lung, spleen, and kidney (Figure 4) showed no evidence for extensive cell injury, even though SWCNT-PEG could be identified within the tissues.

2.3 Behavioral testing

Considering the presence of SWCNT-PEG in the brain cortex, we subjected the animals to the Morris water maze (MWM) to

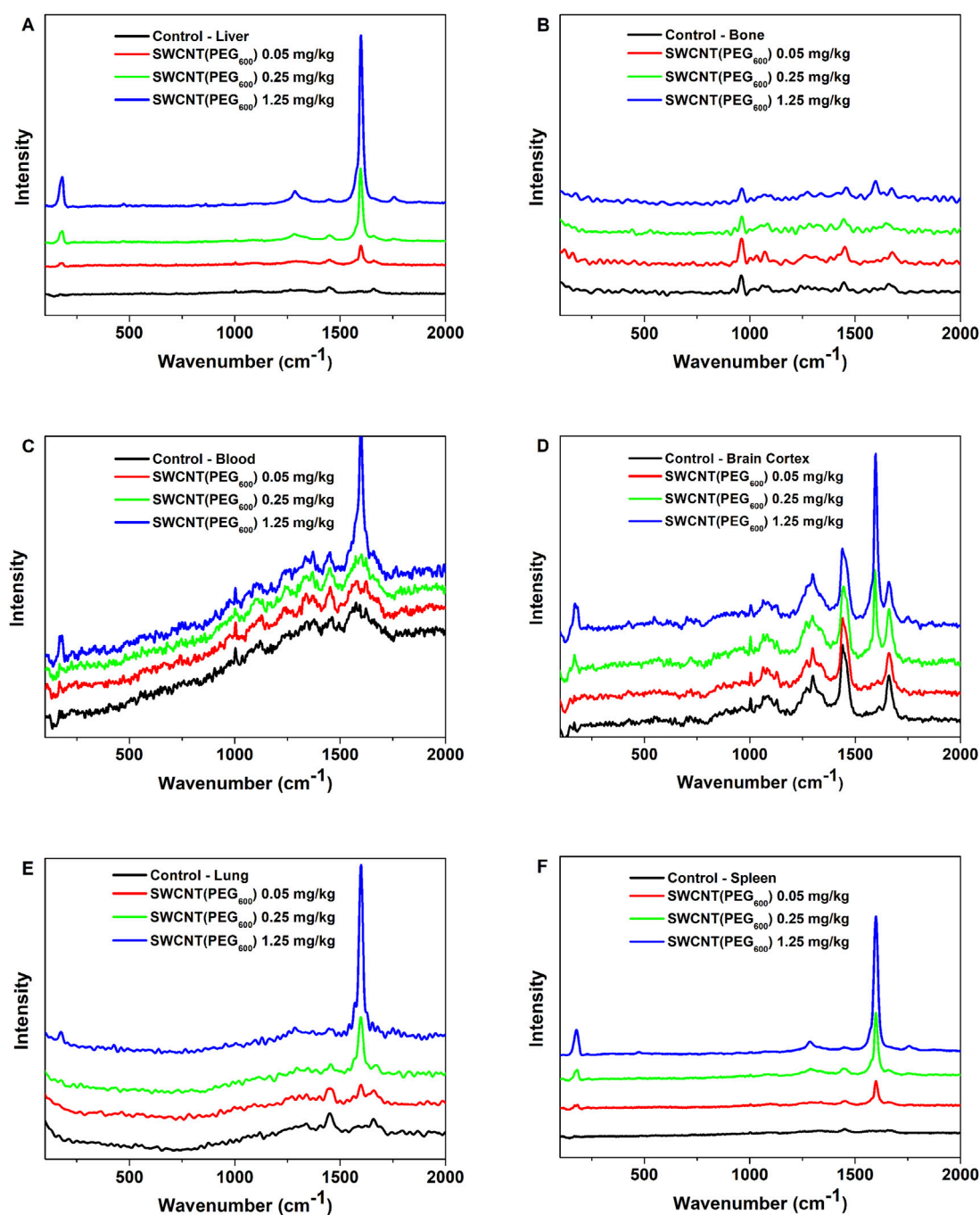


FIGURE 1 Raman spectra of lyophilized tissue samples 24 h after SWCNT-PEG intravenous delivery. Liver (A), bone (B), blood (C), brain cortex (D), lung (E), and spleen (F) after injection of SWCNT-PEG dispersions at different concentrations ($n=5$ per group).

evaluate possible implications of the presence of these nanomaterials in the CNS. The animals were trained for 5 days and were able to learn the task as expected, showing no difference in total traveled distance (Supplementary Figure S3). They were treated with SWCNT-PEG or saline for the last training session, and the test session was performed 24 h later. SWCNT-PEG did not cause impairments in spatial learning 24 h after treatment. Interestingly, the groups treated with the two lowest tested doses showed an improvement in memory

evocation, observed by the time spent in the TQ during the test session (Figure 5).

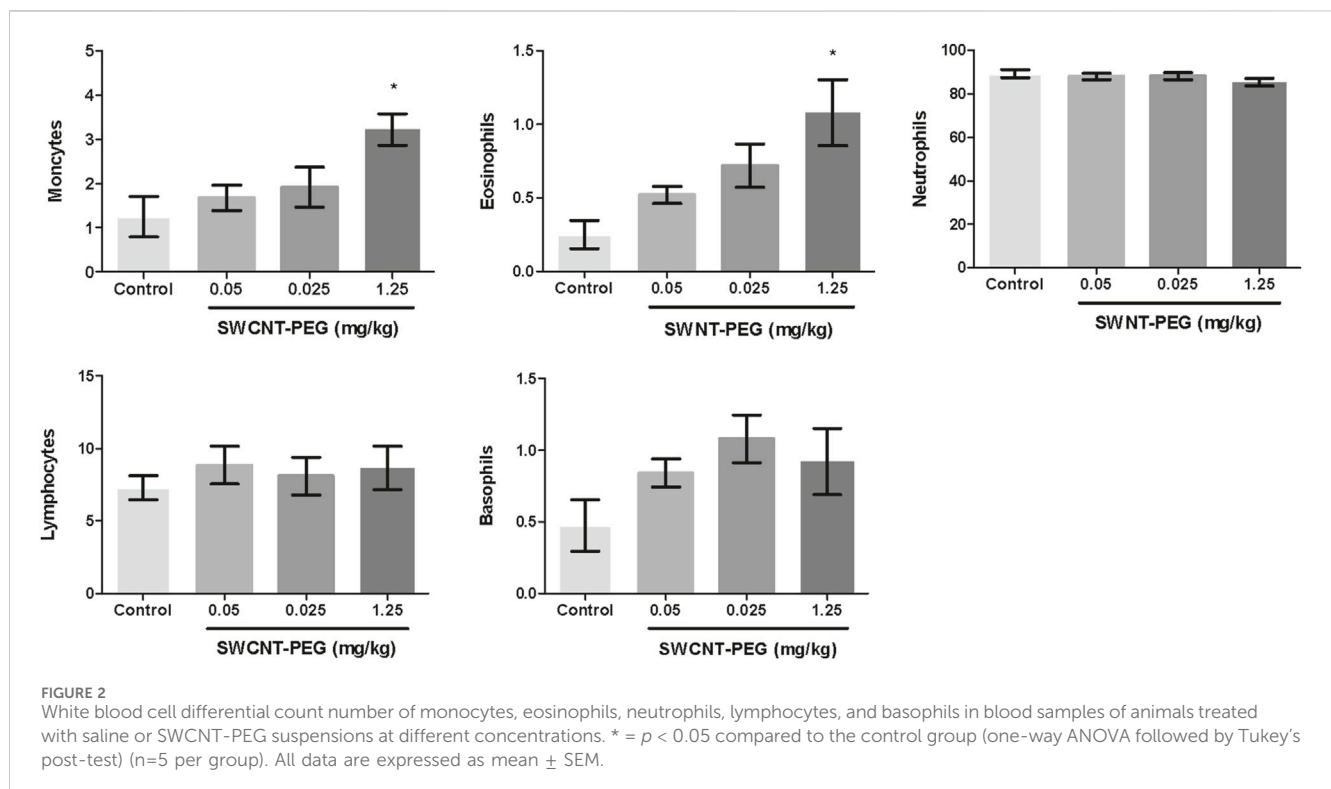
3 Discussion

SWCNT are usually not observable through optical microscopy, but this was possible in the present case because they were found to lodge in the biological tissue in the form of large aggregates. The

TABLE 1 Hematological parameters.

Parameter	Control	SWCNT-PEG 0.05 mg/kg	SWCNT-PEG 0.25 mg/kg	SWCNT-PEG 1.25 mg/kg
RBC ($10^{12}/L$)	8.47 \pm 0.31	8.57 \pm 0.18	7.98 \pm 0.18	8.25 \pm 0.40
HGB (g/L)	15.5 \pm 0.46	15.9 \pm 0.25	14.9 \pm 0.28	15.1 \pm 0.85
MCV (fL)	51.1 \pm 0.39	51.8 \pm 0.38	52.8 \pm 0.51	51.5 \pm 0.57
HCT (%)	43.4 \pm 1.37	44.5 \pm 0.68	42.1 \pm 0.64	42.3 \pm 1.75
MCH (pg)	18.3 \pm 0.20	18.5 \pm 0.18	18.7 \pm 0.18	18.3 \pm 0.23
MCHC (g/L)	35.6 \pm 0.34	35.7 \pm 0.11	35.3 \pm 0.12	35.6 \pm 0.20
PLT ($10^9/L$)	703.2 \pm 42.3	737.0 \pm 53.0	595.4 \pm 45.0	373.2 \pm 78.0 *
MPV (fL)	67.4 \pm 2.7	68.4 \pm 1.3	71.7 \pm 1.8	75.0 \pm 3.4
PCT (%)	0.47 \pm 0.017	0.50 \pm 0.026	0.40 \pm 0.034	0.35 \pm 0.033*
WBC ($10^9/L$)	4.85 \pm 0.72	5.20 \pm 0.58	5.36 \pm 0.40	4.80 \pm 0.60

Red blood counting (RBC), blood count hemoglobin (HGB), mean corpuscular volume (MCV), hematocrit (HCT), mean corpuscular hemoglobin (MCH), mean corpuscular hemoglobin concentration (MCHC), platelet count (PLT), mean platelet volume (MPV), plateletcrit (PCT), and white blood cell count (WBC) from blood samples of animals treated with saline (Control) or different amounts of SWCNT-PEG. * = $p < 0.05$ compared to the control group (one-way ANOVA, followed by Tukey's post-test) (n=5 per group). All data are expressed as mean \pm SEM.



sample used in this experiment was dispersed in water, and the characterization by TEM analysis (Weber et al., 2014) showed that the SWCNT-PEG used in this study were functionalized in bundles (two to five tubes) that were occasionally connected by polymeric masses that presumably led to the formation of larger aggregates. Long periods of bath-sonication were not sufficient to separate the aggregates, which probably become even larger with time. As suggested by the zeta potential of -60 mV and as observed by TEM analysis, the PEGylation of our sample was not homogeneous and was considerably unstable, featuring uncovered portions in the

SWCNT surface that were free to interact with the molecules of the biological medium. This outcome is explainable by the combination of the functionalization method and the length of the PEG chains we used. SWCNTs were subjected to a strong acid treatment for the addition of carboxyl groups, introduced to interact with PEG hydroxyl groups (Sacchetti et al., 2013). It is both possible that some carboxyl groups did not react with PEG (as a result of steric hindrance) and that the PEG chains were not long enough to completely cover the SWCNT surface (Zhao et al., 2005). Thus, not only were the uncovered areas hydrophobic, as is common with

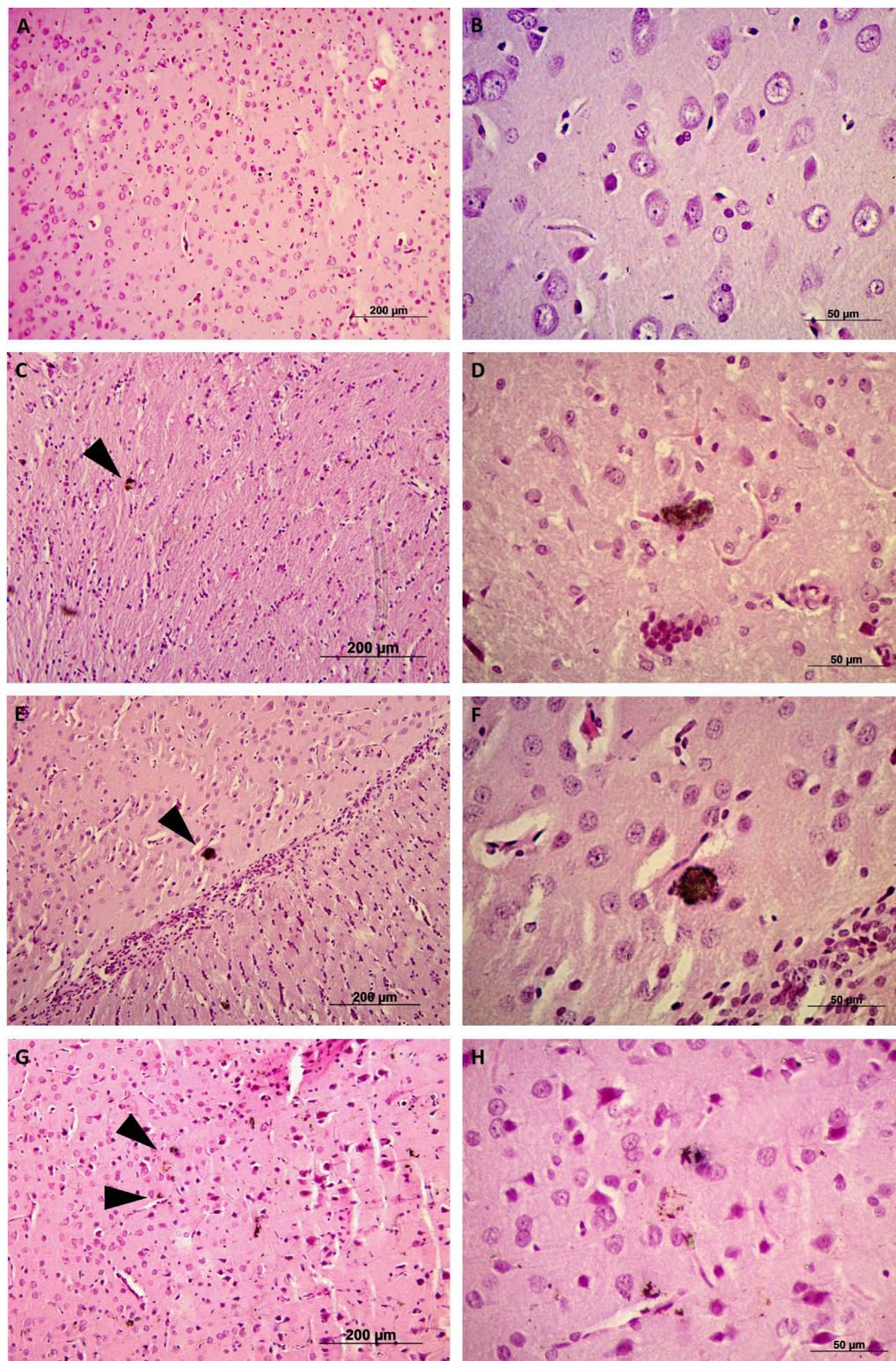


FIGURE 3

Histological analysis of brain tissues from rats injected with a saline solution or SWCNT-PEG dispersions. Representative images of brain coronal sections of control animals (A, B) and animals treated with SWCNT-PEG dispersions at concentrations of 0.05 mg/kg (C, D), 0.25 mg/kg (E, F), or 1.25 mg/kg (G, H) 24 h after infusion. Black arrowheads in C, E, and G indicate the presence of SWCNT-PEG in the tissue parenchyma without signs of cellular or tissue damage. B, D, F, and H micrographs are high-magnification images of specific areas in A, B, C, and D, respectively (n=5 per group).

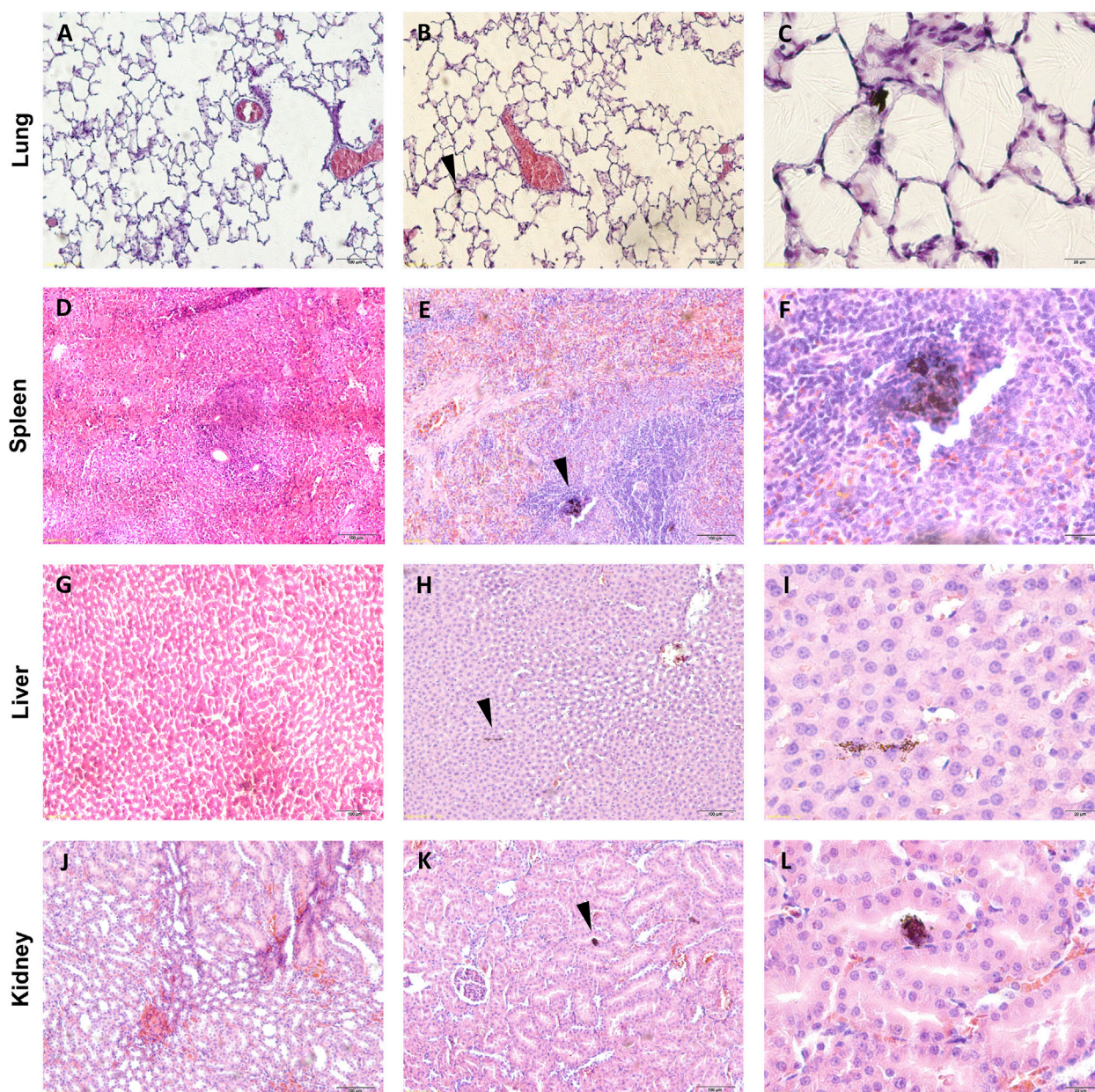
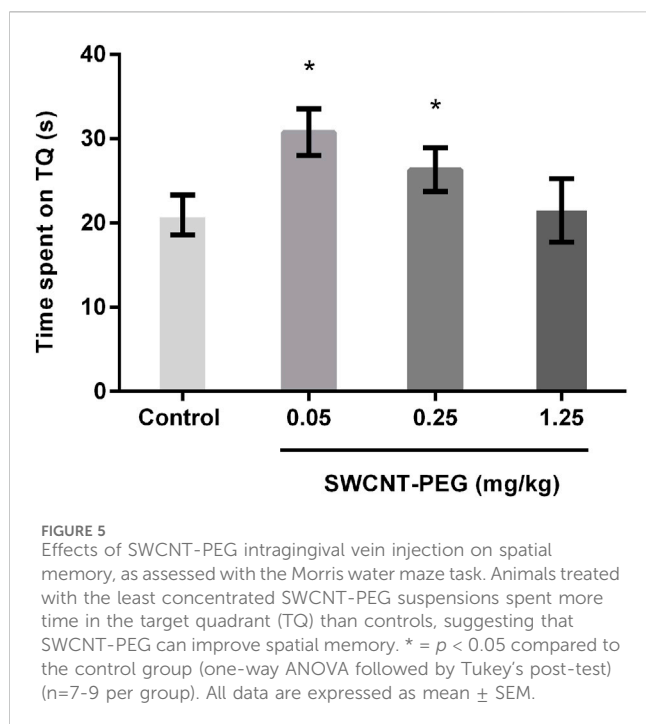


FIGURE 4
 Histological analysis of tissues from rats injected with a saline solution or SWCNT-PEG. Representative images of histological sections of the lung, spleen, liver, and kidney of control animals (**A, D, G, and J**) and animals treated with SWCNT-PEG dispersions at 1.25 mg/kg. Black arrows in (**B, E, H, and K**) indicate the presence of SWCNT-PEG in the tissue parenchyma without signs of cell or tissue damage. (**C, F, I, and L**) are high-magnification micrographs of specific areas in (**B, E, H, and K**) (n = 5 per group).

non-functionalized SWCNT, but they also contained carboxyl groups that were free to interact with the many different molecules present in the biological medium.

Our histological analysis revealed that SWCNT-PEG accumulated in both the liver and the spleen, which can be explained due to opsonization and scavenging by the mononuclear phagocytic system (MPS) (García et al., 2014; Liu et al., 2008). It is well-known that the size, shape, degree, and arrangement of functionalization are important variables for CNT pharmacokinetics, biodistribution, and tissue penetration (Lemos et al., 2023; García et al., 2014; Serpell et al., 2016). As reported by

Liu et al. (2007), PEGylation reduces CNT uptake by the liver and the spleen and increases the blood circulation of SWCNT-PEG5400 (PEG, MW = 5,400 Da), avoiding rapid *in vivo* clearance. Elsewhere, Liu et al. (2008), showed that the PEG chain length and structure (branched or linear) as well as the quality and coverage of PEGylation affect CNT *in vivo* biodistribution. Important characteristics to highlight are the aggregation state of nanotubes in the dispersion. Xue et al. (2016) reported that individualized and aggregated SWCNTs exhibit different bioactivities. They found that the intracranial delivery of aggregated SWCNTs attenuated the increase of extracellular dopamine release induced by



methamphetamine in the ventral striatum through the oxidation of tyrosine and dopamine.

Our results are consistent with these findings and show the presence of SWCNT-PEG in the brain. Al-Jamal et al. (2011) previously showed that MWCNTs were able to successfully deliver siRNA to rat brain cells, confirming direct membrane penetration. Interestingly, we could only detect SWCNT-PEG in the brain cortex (Figure 1D) and not in other brain structures (Supplementary Figure S4). To the best of our knowledge, this is the first report of the biodistribution of SWCNT-PEG in a specific region of the brain tissue after intravenous injection. This raises several questions and hypotheses about the interactions of CNTs with the BBB and specific brain regions. However, it is possible that the SWCNT-PEG went from the bloodstream to the brain parenchyma in regions other than the cerebral cortex but below the detection limit of our methodology. The BBB spreads throughout the brain in a nonhomogeneous fashion, possibly containing regions that are more permeable to the SWCNT-PEG near the cortex. Paviolo et al. (2019) showed the presence of individual SWCNTs (functionalized with phospholipid-polyethylene glycol-PL-PEG) in the CA1 and dentate gyrus (DG) of rat hippocampal organotypic slices and the presence of carbon nanotubes in the cortex, striatum, hippocampus, and ventral midbrain in mouse acute slices either by incubation (organotypic slices) or injection into the cerebral lateral ventricle of live adult mouse (acute slices). This study provides interesting information about the understanding of SWCNT diffusion in different brain extracellular space.

Moreover, Kateb et al. (2007) demonstrated the spontaneous uptake of MWCNTs by the microglia. If SWCNT-PEG of smaller particle size were able to penetrate the brain tissue in other regions, it is possible that the cerebral defenses affected the material, hindering its detection.

Blood analysis revealed an increase in platelets and white blood cells. This observation probably indicates platelet activation resulting from an acute inflammatory response due to the contact of blood cells with SWCNT-PEG (Budak et al., 2016). Although the SWCNTs were pre-coated with PEG in order to form stable dispersions in biological milieu, it has been shown that this does not prevent the activation of the complementary system (Rybak-Smith and Sim, 2011). PEG functionalization did not cover the entire CNT structure, and this uncoated portion was probably almost immediately covered by a corona composed of proteins naturally found in the biological medium which triggers immune responses (Pinals et al., 2020; Yang et al., 2020; Budak et al., 2016; Rybak-Smith and Sim, 2011). Vlasova et al. (2012), demonstrated that these unprotected areas of the CNT may be the primary sites for oxidative damage and the degradation of the nanomaterial. When the immune system recognizes SWCNT-PEG, the first cellular lines of defense of the body, such as monocytes/macrophages and neutrophils (Yang et al., 2019), are among the first to encounter the nanomaterials injected into the blood stream.

The highest SWCNT-PEG dose resulted in monocytosis and eosinophilia. Monocyte activation and inflammation apparently were the first event after the intravenous injection of our SWCNT-PEG. Eosinophil activation is associated with lung dysfunction (such as cystic fibrosis) (Davies et al., 2008) and it is probably related to the biodegradation and clearance of the SWCNT-PEG injected into blood stream that were quickly trapped in the lungs (Vlasova et al., 2012; Ijaz et al., 2023).

To evaluate whether the presence of SWCNT-PEG in the CNS could have led to alterations in behavior, we subjected the animals to the MWM as a method of assessing spatial or place learning. The prefrontal cortex is one of the brain structures involved in learning and memory in this task (Vorhees and Williams, 2006). The MWM has already been used by Yang et al. (2010) as one parameter to evaluate therapeutic effects of SWCNT-acetylcholine in a mouse model for Alzheimer disease. SWCNT-PEG did not lead to behavioral impairments in this task. On the contrary, the animals treated with the two lowest doses showed an improvement in memory evocation according to the tested parameters (more time spent in the target quadrant during the test session). It is important to highlight that, in the biodistribution analysis using Raman spectroscopy, we did not detect the presence of nanotubes in the cerebral cortex at the lowest concentration (0.05 mg/kg). This may be due to the concentration being below the detection limit of the technique, despite the memory improvement observed in the MWM experiment at this dose. Furthermore, at lower nanomaterial concentrations, less aggregation is expected. Consequently, the increased dispersion of nanomaterials may lead to a greater biological effect. However, this possible effect of unknown underlying mechanisms requires further confirmation.

Based on our results, we suggest that the tested nanomaterial can cross the BBB and reach the brain cortex without leading to acute toxicity. These findings encourage the use of SWCNT-PEG in small bundles as a platform for applications in the CNS. Further studies, such as more detailed behavioral tasks, BBB penetration assays, and toxicological tests involving different routes of administration and long-term effects, need to be performed to determine the safest approach for the *in vivo* use of CNT.

4 Materials and methods

4.1 SWCNT-PEG dispersions and characterization

SWCNTs (Sigma-Aldrich, St. Louis, MO, United States) were synthesized by electric arc discharge and functionalized with PEG (MW = 600 Da). SWCNT-PEG preparation was carried out following our previous protocol (Weber et al., 2014). In brief, we prepared the dispersion in deionized water at a high concentration (greater than 2 mg/mL). A multi-step process employing several cycles of sonication, high-shear mixing, centrifugation, and ultracentrifugation was required to prepare a stable dispersion. SWCNT-PEG were previously characterized in another study from our group (Weber et al., 2014) and showed ~25 wt% of grafted PEG, ~60 wt% of SWCNT, and ~20 wt% of 20–40 nm diameter carbon-coated catalyst particles (Ni-Y). As detailed in Weber et al. (2014) and Dal Bosco et al. (2015b), low-resolution TEM analyses showed that this commercial SWCNT-PEG sample formed large aggregates in water even after prolonged bath sonication. The concentration of the final dispersion obtained after the entire process was of approximately 2.1 mg/mL. The Zeta potential of the sample was approximately -60 mV, indicating the presence of many unreacted carboxylic acid groups (-COOH).

4.2 Animals and treatments

Male Wistar rats (2–3 months old, weighing 250–320 g) were purchased from the breeding colony at the Federal University of Rio Grande-FURG (Rio Grande, RS, Brazil) and randomly distributed up to five animals per cage. The animals were kept under standard laboratory conditions (12 h light/dark photoperiod and 23°C ± 1°C) with free access to food pellets and water. The animals were subjected to intralingual vein administration of SWCNT-PEG dispersion (1 mg/mL) at 0.05, 0.25, and 1.25 mg/kg or to saline (control group). Intralingual vein administration was performed under light anesthesia with halothane. The animal was held in a supine position, and the lower lip was retracted to expose the gingiva. A 28–30 gauge needle was then inserted at a 20°–25° angle, approximately 2 mm into the gingiva. (de Oliveira et al., 2009). All procedures were performed according to the guidelines of the Brazilian National Council for the Control of Animal Experimentation (CONCEA) and authorized by the Ethics Committee for Animal Use of the Federal University of Rio Grande-FURG (permission number P006/2014).

4.3 Raman spectroscopy

All animals were killed by decapitation 24 h post-injection, and the organs of interest were carefully removed for biodistribution analysis. Samples were lyophilized, sprayed with mortar, and Raman spectroscopy was performed using a FT-Raman spectrometer (RAM II - Bruker Inc., Karlsruhe, Germany) with excitation source at 1,064 nm (1.16 eV) and 150 mW. This excitation energy is below the self-fluorescence range of the tissues, allowing us to obtain

background-free Raman spectra (Supplementary Figure S1). The characteristic Raman spectrum of SWCNT-PEG in the lyophilized tissues presented peaks approximately 180, 1,300, and 1,600 cm⁻¹, corresponding to RBM, D, and G bands, respectively. The laser excitation energy used was in resonance with the second optical transitions (E22S) of semiconducting SWCNT. All spectra were normalized to the 1,448 cm⁻¹ band, relative to the proteins obtained from the control group.

4.4 Histological analysis

The animals were euthanized and tissues of interest were isolated, fixed in 10% neutral buffered formalin for 12 h at room temperature, and processed according to histological routine. The samples were embedded in paraffin, sectioned at 5 µm, and stained with hematoxylin and eosin (H&E). The sections were observed and examined under a clear field microscope (Zeiss Primo Star) by a certified pathologist (L.A.R.).

4.5 Behavioral assessment

The implications of SWCNT administration on spatial memory were evaluated using the model described by Morris (1984). This Morris water maze (MWM) apparatus consisted of a circular tank divided into four imaginary quadrants and filled with water (24°C ± 1°C) dyed with non-toxic food colorant. A black platform was placed in one of the quadrants (2 cm below water surface level) and visual cues were distributed on the walls of the room. On the first training day, animals were subjected to a four-stage training session (120 s with 70 s interval), starting each stage in a different quadrant. The training sessions were repeated for another 4 days, and the learning progress—time taken to find the platform—was quantified. At the end of the last training session (day 5), the animals received an injection of SWCNT-PEG or saline. On the sixth day, the platform was removed, and the animals were placed in the tank to swim freely for 90 s (test session). Memory consolidation was assessed as the time spent by the animals in the quadrant where the platform was previously placed. Data for this test were acquired using a video tracking system (EthoVision® 3.2, Noldus).

4.6 Hematological and biochemical analysis

Blood was collected 24 h after injection. The rats were euthanized, and blood was collected by cardiac puncture into ethylenediamine tetra acetic acid (EDTA) bottles to evaluate hematological parameters. We performed red blood counting (RBC), blood count hemoglobin (HGB), mean corpuscular volume (MCV), hematocrit (HCT), mean corpuscular hemoglobin (MCH), mean corpuscular hemoglobin concentration (MCHC), platelet count (PLT), mean platelet volume (MPV), plateletcrit (PCT), and white blood cell count (WBC) for monocytes, neutrophils, lymphocytes, eosinophils, and basophils using an automated dialysis machine. For the biochemical analysis, another portion of blood was dispensed into plain bottles, allowed to clot, and centrifuged at 3,500 rpm for 10 min, and the clear sera were

aspirated for biochemical evaluation. Creatinine, alanine aminotransferase (ALT), and aspartate aminotransferase (AST) were analyzed using commercial kits obtained from Doles (Go, Brazil) following the manufacturer's instructions.

4.7 Statistical analysis

Results were analyzed using one-way ANOVA (STATSOFT Statistica, version 7.0) followed by Tukey's *post hoc* test. All data are presented as mean \pm SEM, and *p*-values $<$ 0.05 were considered statistically significant.

5 Conclusions

In this study, we used Raman spectroscopy to detect SWCNT-PEG in the major organs of rats following intravenous administration. The presence of SWCNT-PEG in the liver, bone, blood, lungs, cerebral cortex, and spleen 24 h post-injection was not associated with significant signs of toxicity, as demonstrated by biochemical, histological, and behavioral analyses. These findings are consistent with other studies evaluating the toxicity of PEG-functionalized CNTs. However, certain factors must be considered, such as the length of the PEG chains, the purity of the nanomaterial, and the degree of functionalization. In this study, we utilized a commercial sample of SWCNTs covalently functionalized with PEG (MW = 600 Da), which formed large aggregates in water even after prolonged bath sonication. This aggregation state of the nanotubes in the dispersion may explain why they were observable in biological tissues using optical microscopy, which is uncommon.

Our biodistribution analysis revealed that SWCNT-PEG reached the cerebral cortex but not other brain structures. Despite the presence of these nanomaterials in the CNS, no behavioral impairments were observed in treated animals, as demonstrated by the Morris water maze task. Interestingly, animals injected with the two lowest doses exhibited an improvement in spatial learning based on the tested parameters. This effect on memory evocation was observed even in animals injected with the lowest concentration (0.05 mg/kg), where the SWCNT-PEG Raman signature was not detected. Therefore, we cannot rule out the possibility that this material reached other regions of the brain parenchyma at concentrations below the detection limit of the technique.

This study provides an initial evaluation of the fate and biological effects of PEG-functionalized carbon nanotubes (CNTs) shortly after systemic administration. To achieve a more comprehensive understanding of the safety profile and potential biomedical applications of SWCNT-PEG-based delivery systems, further investigations are required. These should focus on the biodistribution, toxicity, and clearance of these nanomaterials, employing varying dosages, administration routes, and exposure durations.

Data availability statement

The original contributions presented in the study are included in the article/[Supplementary Material](#); further inquiries can be directed to the corresponding author.

Ethics statement

The animal study was approved by Ethics Committee for Animal Use of the Federal University of Rio Grande–FURG (permission number P006/2014). The study was conducted in accordance with the local legislation and institutional requirements.

Author contributions

GB: conceptualization, formal analysis, funding acquisition, investigation, methodology, writing–original draft, writing–review and editing, data curation, and project administration. LD: conceptualization, formal analysis, funding acquisition, investigation, methodology, writing–original draft, and writing–review and editing. AC: data curation, methodology, and writing–original draft. MC: conceptualization, data curation, formal analysis, funding acquisition, investigation, methodology, writing–original draft, and writing–review and editing. SS: formal analysis, investigation, methodology, writing–original draft, and writing–review and editing. CP: funding acquisition, methodology, project administration, and writing–original draft. MK: data curation, formal analysis, methodology, and writing–review and editing. LR: conceptualization, data curation, formal analysis, investigation, methodology, and writing–review and editing. CF: conceptualization, data curation, formal analysis, funding acquisition, investigation, methodology, and writing–review and editing. AS: conceptualization, data curation, formal analysis, funding acquisition, investigation, methodology, project administration, supervision, and writing–review and editing. DB: conceptualization, data curation, formal analysis, funding acquisition, investigation, methodology, project administration, resources, supervision, validation, writing–original draft, and writing–review and editing.

Funding

The authors declare that financial support was received for the research, authorship, and/or publication of this article. This work was partially supported by the Brazilian Institute of Science and Technology (INCT) in Carbon Nanomaterials and the Brazilian agencies Fapemig, CAPES, and CNPq, research grants from Fundação de Amparo à Pesquisa do Estado do Rio Grande do Sul (FAPERGS-PRONEM, process number 11/2037–9), the Nanotoxicology Network (MCTI/CNPq process number 552131/2011–3), and CNPq (Universal, process number 435890/2018–2). Daniela M. Barros, Adelina P. Santos, and Cristiano Fantini were sponsored with productivity research fellowships from the Brazilian National Council of Scientific and Technological Development (CNPq). Gisele Eva Bruch, Lidiane Dal Bosco, and Marcos F. Cordeiro received a graduate scholarship from Coordenação de Aperfeiçoamento de Pessoal de Nível Superior (CAPES). This work was partially supported by the Brazilian Institute of Science and Technology (INCT) in Carbon Nanomaterials—CTI/CNPq/CAPES/FAPs number 16/2014 process number 421701/2017–0.

Acknowledgments

The authors thank the Institute of Science and Technology (INCT) in Carbon Nanomaterials and the Brazilian agencies Fapemig, CAPES, and CNPq for supporting this work, and Beatriz Lopes Tecedor Bassi from Universidade Federal de Minas Gerais (UFMG) for the scientific discussion, contribution to the text, and English correction.

Conflict of interest

The authors declare that the research was conducted in the absence of any commercial or financial relationships that could be construed as a potential conflict of interest.

References

- Al-Jamal, K. T., Gherardini, L., Bardi, G., Nunes, A., Guo, C., Bussy, C., et al. (2011). Functional motor recovery from brain ischemic insult by carbon nanotube-mediated siRNA silencing. *Proc. Natl. Acad. Sci.* 108 (27), 10952–10957. doi:10.1073/pnas.1100930108
- Alshehri, R., Ilyas, A. M., Hasan, A., Arnaout, A., Ahmed, F., and Memic, A. (2016). Carbon nanotubes in biomedical applications: factors, mechanisms, and remedies of toxicity. *J. Med. Chem.* 59, 8149–8167. doi:10.1021/acs.jmedchem.5b01770
- Budak, Y. U., Polat, M., and Huysal, K. (2016). The use of platelet indices, plateletcrit, mean platelet volume and platelet distribution width in emergency non-traumatic abdominal surgery: a systematic review. *Biochem. Medica* 26, 178–193. doi:10.11613/bm.2016.020
- Costa, P. M., Wang, J. T. W., Morfin, J. F., Khanum, T., To, W., Sosabowski, J., et al. (2018). Functionalised carbon nanotubes enhance brain delivery of amyloid-targeting Pittsburgh compound B (PiB)-Derived ligands. *Nanotheranostics* 2 (2), 168–183. doi:10.7150/ntno.23125
- Dal Bosco, L., Weber, G. E., Parfitt, G. M., Cordeiro, A. P., Sahoo, S. K., Fantini, C., et al. (2015a). "Biopersistence of PEGylated carbon nanotubes promotes a delayed antioxidant response after infusion into the rat hippocampus." Editor M. Ahmad, 10. doi:10.1371/journal.pone.0129156
- Dal Bosco, L., Weber, G. E. B., Parfitt, G. M., Paese, K., Gonçalves, C. O. F., Serodre, T. M., et al. (2015b). PEGylated carbon nanotubes impair retrieval of contextual fear memory and alter oxidative stress parameters in the rat hippocampus. *BioMed Res. Int.* 2015, 1–11. doi:10.1155/2015/104135
- Davies, M. J., Hawkins, C. L., Pattison, D. I., and Rees, M. D. (2008). Mammalian heme peroxidases: from molecular mechanisms to health implications. *Antioxidants & Redox Signal.* 10 (7), 1199–1234. doi:10.1089/ars.2007.1927
- de Oliveira, D. T., Souza-Silva, E., and Tonussi, C. R. (2009). Technical report: gingival vein punctation: a new simple technique for drug administration or blood sampling in rats and mice. *Scand. J. Lab. Anim. Sci.* 36 (2), 109–113. doi:10.23675/sjlas.v36i2.174
- Dos Santos, N., Allen, C., Doppen, A. M., Anantha, M., Cox, K. A. K., Gallagher, R. C., et al. (2007). Influence of poly(ethylene glycol) grafting density and polymer length on liposomes: relating plasma circulation lifetimes to protein binding. *Biochimica Biophysica Acta (BBA) - Biomembr.* 1768 (6), 1367–1377. doi:10.1016/j.bbamem.2006.12.013
- Elsaesser, A., and Howard, C. V. (2012). Toxicology of nanoparticles. *Adv. Drug Deliv. Rev.* 64 (2), 129–137. doi:10.1016/j.addr.2011.09.001
- Fernandes, L. F., Bruch, G. E., Massensini, A. R., and Frézard, F. (2018). Recent advances in the therapeutic and diagnostic use of liposomes and carbon nanomaterials in ischemic stroke. *Front. Neurosci.* 12, 453. doi:10.3389/fnins.2018.00453
- García, K. P., Zarschler, K., Barbaro, L., Barreto, J. A., O'Malley, W., Spiccia, L., et al. (2014). Zwitterionic-coated "stealth" nanoparticles for biomedical applications: recent advances in countering biomolecular corona formation and uptake by the mononuclear phagocyte system. *Small* 10 (13), 2516–2529. doi:10.1002/sml.201303540
- Gravely, M., Kindopp, A., Hubert, L., Card, M., Nadeem, A., Miller, C., et al. (2022). Aggregation reduces subcellular localization and cytotoxicity of single-walled carbon nanotubes. *ACS Appl. Mater. Interfaces* 14 (17), 19168–19177. doi:10.1021/acsami.2c02238
- Huang, L., Hu, J., Huang, S., Wang, B., Siaw-Debrah, F., Nyanzu, M., et al. (2017). Nanomaterial applications for neurological diseases and central nervous system injury. *Prog. Neurobiol.* 157, 29–48. doi:10.1016/j.pneurobio.2017.07.003

Publisher's note

All claims expressed in this article are solely those of the authors and do not necessarily represent those of their affiliated organizations, or those of the publisher, the editors, and the reviewers. Any product that may be evaluated in this article, or claim that may be made by its manufacturer, is not guaranteed or endorsed by the publisher.

Supplementary material

The Supplementary Material for this article can be found online at: <https://www.frontiersin.org/articles/10.3389/frcrb.2024.1363919/full#supplementary-material>.

Ijaz, H., Mahmood, A., Abdel-Daim, M. M., Sarfraz, R. M., Zaman, M., Zafar, N., et al. (2023). Review on carbon nanotubes (CNTs) and their chemical and physical characteristics, with particular emphasis on potential applications in biomedicine. *Inorg. Chem. Commun.* 155, 111020. doi:10.1016/j.inoche.2023.111020

Irudayanathan, F. J., Trasatti, J. P., Karande, P., and Nangia, S. (2016). Molecular architecture of the blood brain barrier tight junction proteins--A synergistic computational and *in vitro* approach. *J. Phys. Chem. B* 120 (1), 77–88. doi:10.1021/acs.jpcc.5b09977

Iverson, N. M., Barone, P. W., Shandell, M., Trudel, L. J., Sen, S., Sen, F., et al. (2013). *In vivo* biosensing via tissue localizable near infrared fluorescent single walled carbon nanotubes. *Nat. Nanotechnol.* 8 (11), 873–880. doi:10.1038/nnano.2013.222

Kafa, H., Wang, J. T. W., Rubio, N., Klippstein, R., Costa, P. M., Hassan, HAFM, et al. (2016). Translocation of LRP1 targeted carbon nanotubes of different diameters across the blood-brain barrier *in vitro* and *in vivo*. *J. Control. Release* 225, 217–229. doi:10.1016/j.jconrel.2016.01.031

Kafa, H., Wang, J. T. W., Rubio, N., Venner, K., Anderson, G., Pach, E., et al. (2015). The interaction of carbon nanotubes with an *in vitro* blood-brain barrier model and mouse brain *in vivo*. *Biomaterials* 53, 437–452. doi:10.1016/j.biomaterials.2015.02.083

Kateb, B., Van Handel, M., Zhang, L., Bronikowski, M. J., Manohara, H., and Badie, B. (2007). Internalization of MWCNTs by microglia: possible application in immunotherapy of brain tumors. *NeuroImage* 37, S9–S17. doi:10.1016/j.neuroimage.2007.03.078

Kavosi, A., Hosseini Ghale Noei, S., Madani, S., Khalighfard, S., Khodayari, S., Khodayari, H., et al. (2018). RETRACTED ARTICLE: the toxicity and therapeutic effects of single-and multi-wall carbon nanotubes on mice breast cancer. *Sci. Rep.* 8 (1), 8375. doi:10.1038/s41598-018-26790-x

Khongkow, M., Yata, T., Boonrunsiman, S., Ruktanonchai, U. R., Graham, D., and Namdee, K. (2019). Surface modification of gold nanoparticles with neuron-targeted exosome for enhanced blood-brain barrier penetration. *Sci. Rep.* 9 (1), 8278. doi:10.1038/s41598-019-44569-6

Lee, H. J., Park, J., Yoon, O. J., Kim, H. W., Lee, D. Y., Kim, D. H., et al. (2011). Amine-modified single-walled carbon nanotubes protect neurons from injury in a rat stroke model. *Nat. Nanotechnol.* 6 (2), 121–125. doi:10.1038/nnano.2010.281

Lemos, J. d. A., Soares, D. C. F., Pereira, N. C., Gomides, L. S., Silva, J. d. O., Bruch, G. E., et al. (2023). Preclinical evaluation of PEG-Multiwalled carbon nanotubes: radiolabeling, biodistribution and toxicity in mice. *J. Drug Deliv. Sci. Technol.* 86, 104607. doi:10.1016/j.jddst.2023.104607

Liu, Z., Cai, W., He, L., Nakayama, N., Chen, K., Sun, X., et al. (2007). *In vivo* biodistribution and highly efficient tumour targeting of carbon nanotubes in mice. *Nat. Nanotechnol.* 2 (1), 47–52. doi:10.1038/nnano.2006.170

Liu, Z., Davis, C., Cai, W., He, L., Chen, X., and Dai, H. (2008). Circulation and long-term fate of functionalized, biocompatible single-walled carbon nanotubes in mice probed by Raman spectroscopy. *Proc. Natl. Acad. Sci. U. S. A.* 105 (5), 1410–1415. doi:10.1073/pnas.0707654105

Mann, F. A., Galonska, P., Herrmann, N., and Kruss, S. (2022). Quantum defects as versatile anchors for carbon nanotube functionalization. *Nat. Protoc.* 17 (3), 727–747. doi:10.1038/s41596-021-00663-6

Metternich, J. T., Sistemich, L., Niffler, R., Herberich, S., and Kruss, S. (2023). Rational design of near-infrared fluorescent carbon nanotube biosensors with covalent DNA-anchors. *ChemRxiv* 27. doi:10.26434/chemrxiv-2023-838d6

- Morris, R. (1984). Developments of a water-maze procedure for studying spatial learning in the rat. *J. Neurosci. Methods* 11 (1), 47–60. doi:10.1016/0165-0270(84)90007-4
- Nunes, A., Bussy, C., Gherardini, L., Meneghetti, M., Herrero, M. A., Bianco, A., et al. (2012). *In vivo* degradation of functionalized carbon nanotubes after stereotactic administration in the brain cortex. *Nanomedicine* 7 (10), 1485–1494. doi:10.2217/nnm.12.33
- Pardridge, W. M. (2012). Drug transport across the blood-brain barrier. *J. Cereb. Blood Flow & Metabolism* 32 (11), 1959–1972. doi:10.1038/jcbfm.2012.126
- Paviolo, C., Soria, F. N., Ferreira, J. S., Lee, A., Groc, L., Bezdard, E., et al. (2019). Nanoscale exploration of the extracellular space in the live brain by combining single carbon nanotube tracking and super-resolution imaging analysis. *Methods San. Diego Calif.* doi:10.1016/j.ymeth.2019.03.005
- Pinals, R. L., Yang, D., Rosenberg, D. J., Chaudhary, T., Crothers, A. R., Iavarone, A. T., et al. (2020). Quantitative protein corona composition and dynamics on carbon nanotubes in biological environments. *Angew. Chem. Int. Ed.* 59 (52), 23668–23677. doi:10.1002/anie.202008175
- Rybak-Smith, M. J., and Sim, R. B. (2011). Complement activation by carbon nanotubes. *Adv. Drug Deliv. Rev.* 63 (12), 1031–1041. doi:10.1016/j.addr.2011.05.012
- Sacchetti, C., Motamedchaboki, K., Magrini, A., Palmieri, G., Mattei, M., Bernardini, S., et al. (2013). Surface polyethylene glycol conformation influences the protein corona of polyethylene glycol-modified single-walled carbon nanotubes: potential implications on biological performance. *ACS Nano* 7 (3), 1974–1989. doi:10.1021/nn400409h
- Serpell, C. J., Kostarelos, K., and Davis, B. G. (2016). Can carbon nanotubes deliver on their promise in biology? Harnessing unique properties for unparalleled applications. *ACS Cent. Sci.* 2 (4), 190–200. doi:10.1021/acscentsci.6b00005
- Soligo, M., Felsani, F. M., Da Ros, T., Bosi, S., Pellizzoni, E., Bruni, S., et al. (2021). Distribution in the brain and possible neuroprotective effects of intranasally delivered multi-walled carbon nanotubes. *Nanoscale Adv.* 3 (2), 418–431. doi:10.1039/d0na00869a
- Son, M., Mehra, P., Nguyen, F. T., Jin, X., Koman, V. B., Gong, X., et al. (2023). Molecular recognition and *in vivo* detection of temozolomide and 5-Aminoimidazole-4-carboxamide for glioblastoma using near-infrared fluorescent carbon nanotube sensors. *ACS Nano* 17 (1), 240–250. doi:10.1021/acsnano.2c07264
- Tam, V. H., Sosa, C., Liu, R., Yao, N., and Priestley, R. D. (2016). Nanomedicine as a non-invasive strategy for drug delivery across the blood brain barrier. *Int. J. Pharm.* 515 (1–2), 331–342. doi:10.1016/j.ijpharm.2016.10.031
- Vlasova, I. I., Vakhrusheva, T. V., Sokolov, A. V., Kostevich, V. A., Gusev, A. A., Gusev, S. A., et al. (2012). PEGylated single-walled carbon nanotubes activate neutrophils to increase production of hypochlorous acid, the oxidant capable of degrading nanotubes. *Toxicol. Appl. Pharmacol.* 264 (1), 131–142. doi:10.1016/j.taap.2012.07.027
- Vorhees, C. V., and Williams, M. T. (2006). Morris water maze: procedures for assessing spatial and related forms of learning and memory. *Nat. Protoc.* 1 (2), 848–858. doi:10.1038/nprot.2006.116
- Weber, G. E. B., Dal Bosco, L., Gonçalves, C. O. F., Santos, A. P., Fantini, C., Furtado, C. A., et al. (2014). Biodistribution and toxicological study of PEGylated single-wall carbon nanotubes in the zebrafish (*Danio rerio*) nervous system. *Toxicol. Appl. Pharmacol.* 280 (3), 484–492. doi:10.1016/j.taap.2014.08.018
- Xue, X., Yang, J. Y., He, Y., Wang, L. R., Liu, P., Yu, L. S., et al. (2016). Aggregated single-walled carbon nanotubes attenuate the behavioural and neurochemical effects of methamphetamine in mice. *Nat. Nanotechnol.* 11 (7), 613–620. doi:10.1038/nnano.2016.23
- Yang, D., Yang, S. J., Del Bonis-O'Donnell, J. T., Pinals, R. L., and Landry, M. P. (2020). Mitigation of carbon nanotube neurosensor induced transcriptomic and morphological changes in mouse microglia with surface passivation. *ACS Nano* 14 (10), 13794–13805. doi:10.1021/acsnano.0c06154
- Yang, M., Zhang, M., Nakajima, H., Yudasaka, M., Iijima, S., and Okazaki, T. (2019). Time-dependent degradation of carbon nanotubes correlates with decreased reactive oxygen species generation in macrophages. *Int. J. Nanomedicine* 14, 2797–2807. doi:10.2147/ijn.s199187
- Yang, S. tao, Guo, W., Lin, Y., Deng, X. y., Wang, H. f., Sun, H. f., et al. (2007). Biodistribution of pristine single-walled carbon nanotubes *in vivo*. *J. Phys. Chem. C* 111 (48), 17761–17764. doi:10.1021/jp070712c
- Yang, Z., Zhang, Y., Yang, Y., Sun, L., Han, D., Li, H., et al. (2010). Pharmacological and toxicological target organelles and safe use of single-walled carbon nanotubes as drug carriers in treating Alzheimer disease. *Nanomedicine Nanotechnol. Biol. Med.* 6 (3), 427–441. doi:10.1016/j.nano.2009.11.007
- Zhao, B., Hu, H., Yu, A., Perea, D., and Haddon, R. C. (2005). Synthesis and characterization of water soluble single-walled carbon nanotube graft copolymers. *J. Am. Chem. Soc.* 127 (22), 8197–8203. doi:10.1021/ja042924i
- Zhu, Z. (2017). An overview of carbon nanotubes and graphene for biosensing applications. *Nano-Micro Lett.* 9 (3), 25. doi:10.1007/s40820-017-0128-6